Desalination and Water Treatment
www.deswater.com

doi: 10.5004/dwt.2017.21654

97 (2017) 14–22
November

Analysis of silica fouling in membrane distillation using response surface methodology

Yongsun Jang, Hyeongrak Cho, Yonghyun Shin, Jihyeok Choi, Younghoon Ko, Yongjun Choi, Sangho Lee*

School of Civil and Environmental Engineering, Kookmin University, Jeongneung-Dong, Seongbuk-Gu, Seoul 136-702, Korea, Tel. +822 910 4529; Fax: +822 910 4939; emails: sanghlee@kookmin.ac.kr (S. Lee), jjayo0907@gmail.com (Y. Jang)

Received 27 August 2017; Accepted 28 October 2017

ABSTRACT

Membrane distillation (MD) is a promising technology in the production of pure water from saline water or wastewater. Although MD has various attractive advantages compared with traditional desalination techniques, fouling is one of the main issues that should be resolved for long-term operation and its commercialization. Therefore, this study intends to understand the behaviors of colloidal silica fouling. Using model solution containing colloidal silica in the presence of NaCl, a series of experiments were carried out. Based on response surface methodology, second-order polynomial model, which can predict fouling ratios (J/J_0), was developed and the effect of each factor on fouling was analyzed with flux patterns and scanning electron microscopic images. Severe silica cake layers were formed on the membrane surfaces in high ionic strength conditions and various flux tendencies were observed according to the change of factors.

Keywords: Membrane distillation; Response surface methodology; Silica; Fouling; Prediction

1. Introduction

The water shortage has become one of the most critical problems all over the world. Although there is a lot of water available as a form of seawater, it cannot be directly used due to its high salt concentration. This has led to the development of technologies to convert seawater to freshwater. Membrane desalination is one of the approaches that have been widely explored to conquer the challenge of increasing demand of clean water [1–5].

Membrane distillation (MD), which is based on a separation mechanism driven by thermal energy, is one of novel technologies for desalination. MD employs hydrophobic microporous filters, where it only allows the passage of water vapor through the membrane and blocks the penetration of liquid water. Water evaporates from hot feed side through membrane and condenses at the cold permeated side. In this way, collecting purified water is achieved from various feed waters containing either salts or pollutants [6–9]. MD has several advantages compared with other membrane technologies. These include operation at mild conditions, reduction of operational or capital costs using low grade waste heat, theoretically 100% rejection of particulates and non-volatile solutes, less sensitive to membrane fouling, the ability to treat high salinity water such as RO brine, and allowing zero discharge of concentrated brine [10,11].

Nevertheless, MD has not been widely accepted by industry because of several limitations. One of them is membrane fouling, which is a critical issue to be resolved prior to long-term operations and commercial applications. A number of studies have been conducted about the fouling mechanism of traditional desalination technology such as RO and NF [12–17]. However, behaviors of MD fouling are still not well understood in many cases. Due to the differences in membrane structures and operating conditions,

* Corresponding author.

the fouling mechanism in MD should not be similar to those in other membrane processes [6,18,19]. MD fouling results from particle deposition, organic adsorption, biofouling, and scale formation [20]. Accumulation of sparingly soluble salts such as $CaSO_4$, $CaCO_3$, and silica leads to the scale formation. Crystals formed by scaling can reduce pure water flux by hindering mass transport of vapor and bring wetting problem by lessening hydrophobicity [6,20–24].

Of particular interest in this work is silica fouling in MD. In natural water, dissolved silica exists either as crystalline or amorphous form. The formation of silica scale is dependent on the pH of the solution. Factors affecting the formation of silica scale include the size and shape, surface charge, and interactions with ions in the feed solution. In addition, fluid viscosity is affected by temperature of feed solution where silica dissolved [22,25–27]. Therefore, silica fouling behaviors are complex due to the combinations of these factors.

This study aims at better understanding of silica fouling in MD based on response surface methodology (RSM). The RSM includes statistical design of experiments and it is widely used for developing a mathematical model for prediction of the output responses [22,28,29]. Using RSM, second-order polynomial model that predict the extent of fouling was derived. When designing RSM, fouling ratio (J/J_0) (Y) was set to be response of the result and concentration of silica (X_1), NaCl (X_2), and temperature difference (X_3) between feed and permeate (dT) were set to be variables. Moreover, in order to confirm the impact of the presence of NaCl on silica cake layers formation, fouled membrane surfaces were observed using scanning electron microscopy (SEM). With flux graphs and response surfaces, analysis on influence of each variable on silica fouling behaviors was carried out.

2. Materials and methods

2.1. Preparation of feed solution

As a model foulant, colloidal silica (SNOWTEX, ST-ZL) was used for fouling experiments. Particle size of the silica is 70–100 nm and percentage concentration of the original solution is 40–41 wt%. Colloidal silica was diluted by deionized (DI) water according to target concentration and NaCl (Sigma-Aldrich, Korea) also was added to the silica solution. Silica concentration was determined from 1,000 to 9,000 mg/L and NaCl concentration was from 5,000 to 45,000 mg/L. In every experiment, 1 L volume of feed water was used.

2.2. RSM design

The RSM was applied to analyze silica fouling behaviors and develop experimental model equations that can predict reduction of flux by normalized flux. In RSM design, concentration of 'silica', 'NaCl' and 'temperature differences' between feed and permeate was set to be X_1, X_2, and X_3, respectively, as variables which have impact on membrane fouling. The response (Y) was fouling ratio. To derive RSM model equation, totally 20 runs of fouling experiments were carried out with different experimental conditions, which are summarized in Tables 1 and 2. When analyzing RSM, α value was set to be 0.95.

Table 1
Variables and responses design for RSM analysis

Run order	X_1 (silica) (mg/L)	X_2 (NaCl) (mg/L)	X_3 (dT) (°C)
–1.68	1,000	5,000	35
–1	3,000	15,000	40
0	5,000	25,000	45
1	7,000	35,000	50
1.68	9,000	45,000	55

From the analysis of variance, a second polynomial model can be developed as shown below [22,29].

$$Y_k = \beta_{k0} + \sum_{i=1}^{4} \beta_{ki} X_i + \sum_{i=1}^{3} \sum_{j=i+1}^{4} \beta_{kij} X_i X_j + \sum_{i=1}^{4} \beta_{kii} X_i^2 \quad (1)$$

where Y_k is the fouling ratio meaning normalized flux at finish point of experiments and X_i is designated as foulants concentration and temperature differences. The R^2 was evaluated for the assessment of the accuracy of the model.

2.3. Laboratory MD system

Fig. 1 shows a laboratory-scale direct contact membrane distillation (DCMD) experimental setup. In this system, two main water streams exist: hot feed water which was heated directly by a hotplate at bottom of the flask and cold permeate water condensed during the experiments by passing through a chiller. The temperature of the chiller was maintained at 20°C by circulating water with a water bath. The flow rates of the feed and permeate were 0.6 and 0.4 L/min, respectively, and were distributed by gear pumps (Micro Gear Pump, USA). The feed was stirred during the whole operation time by a magnetic bar in the feed tank. All fouling tests were carried out during the operation time of 9 h. The mass of the permeate was measured using a digital balance (OHAUS, USA) and the measured value was transmitted to a personal computer in every minute.

2.4. MD membranes and module

Hydrophobic flat sheet microfiltration membranes (Milipore, USA) with the nominal pore size of 0.22 μm were used for MD tests. The effective membrane area was 0.0012 m^2 (2 cm × 6 cm). The schematic diagram of module is shown in Fig. 2. The MD module was made of acryl and the length, width, and depth of the channel were 60, 20, and 2 mm, respectively. The feed water passed through the upper part of module and permeate passed through the bottom part. The feed and permeate were in opposite direction (counter current flow).

3. Results and discussion

3.1. Membrane performance tests

Prior to fouling experiments, the performance of the intrinsic membrane was tested using DI water for 1 h. The results are summarized in Table 3. Experiments proceeded with temperature difference between feed and permeate

Table 2
Variables and responses design for RSM analysis

Run order	X_1 (silica)	X_2 (NaCl)	X_3 (dT)
1	–1.00 (3,000 mg/L)	–1.00 (15,000 mg/L)	–1.00 (40°C)
2	–1.00 (3,000 mg/L)	1.00 (35,000 mg/L)	–1.00 (40°C)
3	1.00 (7,000 mg/L)	1.00 (35,000 mg/L)	–1.00 (40°C)
4	0.00 (5,000 mg/L)	0.00 (25,000 mg/L)	0.00 (45°C)
5	1.00 (7,000 mg/L)	1.00 (35,000 mg/L)	1.00 (50°C)
6	1.00 (7,000 mg/L)	–1.00 (15,000 mg/L)	1.00 (50°C)
7	0.00 (5,000 mg/L)	0.00 (25,000 mg/L)	0.00 (45°C)
8	1.00 (7,000 mg/L)	–1.00 (15,000 mg/L)	–1.00 (40°C)
9	–1.00 (3,000 mg/L)	1.00 (35,000 mg/L)	1.00 (50°C)
10	–1.68 (1,000 mg/L)	0.00 (25,000 mg/L)	0.00 (45°C)
11	0.00 (5,000 mg/L)	0.00 (25,000 mg/L)	–1.68 (35°C)
12	0.00 (5,000 mg/L)	–1.68 (5,000 mg/L)	0.00 (45°C)
13	0.00 (5,000 mg/L)	0.00 (25,000 mg/L)	0.00 (45°C)
14	0.00 (5,000 mg/L)	0.00 (25,000 mg/L)	0.00 (45°C)
15	0.00 (5,000 mg/L)	0.00 (25,000 mg/L)	1.68 (55°C)
16	–1.00 (3,000 mg/L)	–1.00 (15,000 mg/L)	1.00 (50°C)
17	0.00 (5,000 mg/L)	0.00 (25,000 mg/L)	0.00 (45°C)
18	0.00 (5,000 mg/L)	0.00 (25,000 mg/L)	0.00 (45°C)
19	1.68 (9,000 mg/L)	0.00 (25,000 mg/L)	0.00 (45°C)
20	0.00 (5,000 mg/L)	1.68 (45,000 mg/L)	0.00 (45°C)
Y_1	Fouling ratio		

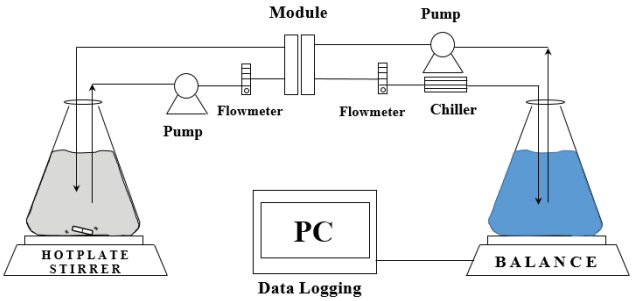

Fig. 1. Laboratory DCMD experimental setup.

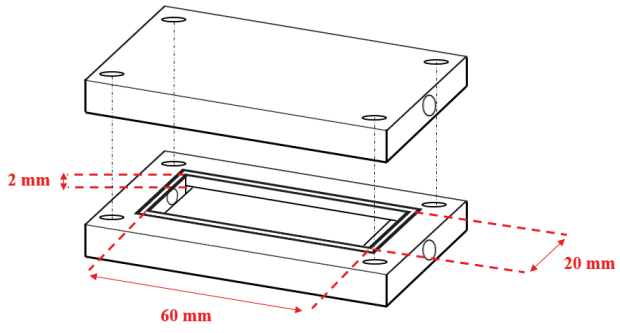

Fig. 2. Schematic diagram of DCMD module.

Table 3
Results of membrane performance tests

dT (°C)	Flux (LMH)
35	15
40	19.5
45	24
50	29.5
55	36

from 35°C to 55°C at interval of 5°C and temperature of permeate was fixed at 20°C. At these conditions, pure water fluxes were from 15 to 36 LMH. The following empirical equation was obtained to express water flux as a function of the temperature difference with the R^2 of 0.9993.

$$J = 0.163(dT)^{1.9188} \quad (2)$$

3.2. DCMD fouling experiments with single foulant

The change of flux during MD operation using feed solution containing only silica is shown in Fig. 3(a). Although the silica concentration was high (5,000 mg/L), no flux decline was observed. Similar result was obtained using feed solution containing only NaCl of 25,000 mg/L (Fig. 3(a)). Also, the results were similar to that using DI water as the feed solution.

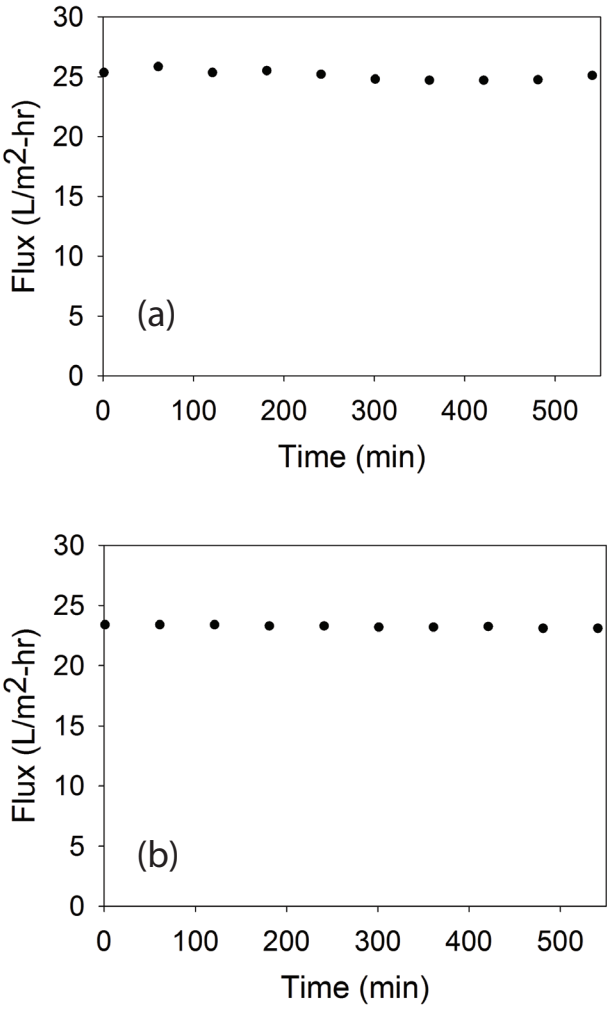

Fig. 3. Dependence of flux on time during MD experiments using (a) silica 5,000 mg/L and (b) NaCl 25,000 mg/L at d*T* 45°C.

These results may be attributed to electrical repulsive force existing between colloidal silica and the membrane. As the surfaces of the silica and membrane are negatively charged, it is difficult to have silica deposition on the membrane surface. Even if the silica cake layers are formed, they may be highly porous due to the repulsive force.

After the fouling experiments, membrane surfaces were examined by SEM and Fig. 4 shows the images. The SEM results suggest that both silica and NaCl did not cause serious fouling. Although silica cakes or NaCl crystal particles existed on the membrane surface, they did not cover the entire surface and there were still many open pores. This implies that their effects on flux are negligible as shown in Fig. 3.

3.3. Fouling by mixed solution with silica and NaCl

Although silica in DI water may not cause MD fouling due to its high surface charge, it may result in fouling in a solution with a high salt concentration. At high ionic strength, electrostatic repulsive force decreases. Therefore, it is important to elucidate the effect of ionic strength (or salt

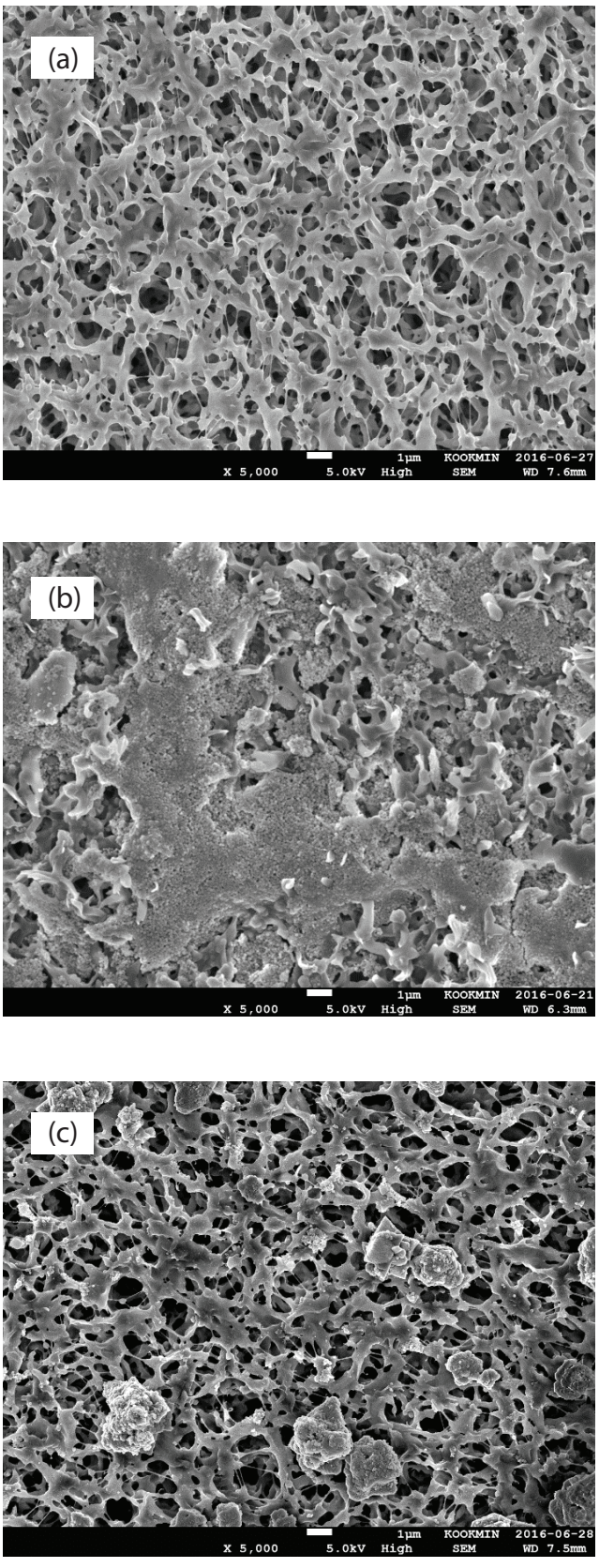

Fig. 4. SEM images of membrane surfaces of (a) clean membrane, (b) after experiment using silica 5,000 mg/L, and (c) after experiment using NaCl 25,000 mg/L.

concentration) on silica fouling in MD. For this purpose, the RSM was applied to obtain a quantitative relationship.

According to the RSM design, experiments were conducted with the solutions containing both silica and NaCl in various concentration and temperature conditions. Table 4 shows the results of fouling ratios according to run order. Unlike the results of single foulant (Fig. 3), severe flux decline was observed in some cases and the range of fouling ratios was from 0.25 to 0.95. It is evident from the results that the NaCl concentration (and ionic strength) significantly affects the extent of silica fouling.

Fig. 5 shows the SEM image of the membrane surfaces fouled by silica 9,000 mg/L and NaCl 25,000 mg/L at 45°C of temperature difference. It looks quite different from the result in Fig. 4(b), which is the SEM image after the MD operation using the feed solution containing only silica of 5,000 mg/L. Thick and dense cake layers cover the entire membrane surface, which caused 60% of flux reduction (run order-19). This fouling mechanism can be explained by Derjaguin–Landau–Vervey–Overbeek (DLVO) theory. According to DLVO theory, repulsive energy between particles is reduced at higher ionic strength solution and therefore energy barrier decreases, resulting in not only particle aggregation but also attachment of particles on the membrane [27]. Accordingly, it is evident that ionic strength has great effect on formation of silica cake layers.

3.4. Development of model equation using response surface method

After the fouling experiments, the analysis of RSM was carried out to derive regression model to predict fouling ratio based on the results of fouling ratio and initial flux. The confidential level was set to be 95%. As mentioned above, the regression model is a function of concentration of silica and NaCl and temperature differences between feed and permeate (dT). Using statistical method with experimental datum, regression model could be developed that can predict the fouling ratio in MD operation and the coefficients and p values are summarized in Table 5. The model had 91.77% of R^2 which means the model calculations are reasonable. All of the p values were less than 0.05 except for B_{11}, B_{33}, and B_{23}, indicating that these models properly describe the functional relationship between the experimental factors and the response variable. Especially, p value of B_{33} is much great indicating the term of square of dT had a negligible impact on silica cake formation. Based on the results, second-order polynomial models can be presented as below:

Table 4
Fouling ratios according to run order designed by RSM

Run order	Y (fouling ratio (J/J_0))
1 (–1, –1, –1)	0.87
2 (–1, 1, –1)	0.61
3 (1, 1, –1)	0.46
4 (0, 0, 0)	0.50
5 (1, 1, 1)	0.25
6 (1, –1, 1)	0.50
7 (0, 0, 0)	0.51
8 (1, –1, –1)	0.76
9 (–1, 1, 1)	0.58
10 (–1.68, 0, 0)	0.86
11 (0, 0, –1.68)	0.66
12 (0, –1.68, 0)	0.95
13 (0, 0, 0)	0.50
14 (0, 0, 0)	0.51
15 (0, 0, 1.68)	0.42
16 (–1, –1, 1)	0.71
17 (0, 0, 0)	0.55
18 (0, 0, 0)	0.52
19 (1.68, 0, 0)	0.41
20 (0, 1.68, 0)	0.48

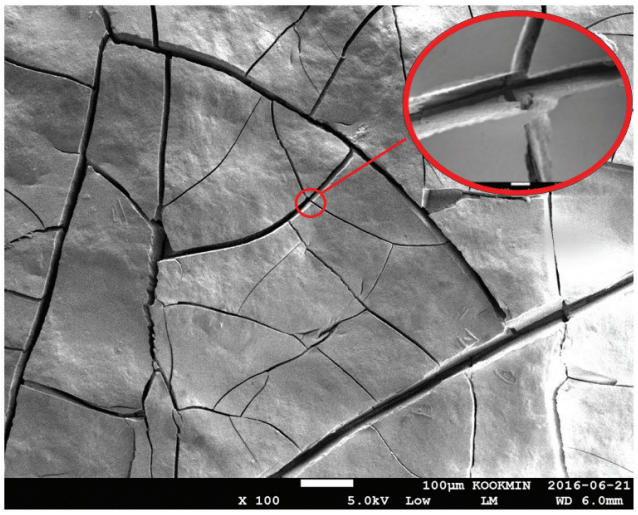

Fig. 5. The SEM image of membrane surfaces after MD experiment in the following operation condition: silica 9,000 mg/L and NaCl 25,000 mg/L at dT 45°C.

Table 5
Coefficients and p value of polynomial regression model for responses

	Y (fouling ratio (J/J_0))	
	Coefficient	p Value
B_0 (constant)	0.516436	0.000
B_1 (silica)	–0.0978854	0.000
B_2 (NaCl)	–0.126709	0.000
B_3 (dT)	–0.0778825	0.000
B_{11} (silica × silica)	0.0330409	0.031
B_{22} (NaCl × NaCl)	0.0613252	0.001
B_{33} (dT × dT)	–5.46654E–04	0.968
B_{12} (silica × NaCl)	–0.0475000	0.023
B_{13} (silica × dT)	–0.0625000	0.005
B_{23} (NaCl × dT)	0.0225000	0.232
R^2	91.77%	

$$Y = 0.516436 - 0.0978854X_1 - 0.126709X_2 - 0.0778825X_3 + 0.0330409X_1^2 + 0.0613252X_2^2 - 0.0475X_1X_2 - 0.0625X_1X_3 \quad (3)$$

3.5. Analysis of fouling behaviors by flux patterns

Although conditions of experiments designed for RSM analysis do not have a set of rules to analyze fouling behaviors by a specific foulant, some comparable cases were used to find the effect on fouling in each variable. Fig. 6 presents flux patterns with respect to operating time. In Fig. 6(a), silica concentration was changed from 3,000 to 7,000 mg/L and NaCl concentration was changed from 15,000 to 35,000 mg/L at 40°C of dT. Fouling ratios changed more sensitively to NaCl concentration than silica concentration. The fouling ratio changed from 10% to 14% by changing silica concentration from 3,000 to 7,000 mg/L. On the other hand, the fouling ratio changed from 26% to 30% by changing NaCl concentration from 15,000 to 35,000 mg/L.

Fig. 6(b) shows the effect of change in concentration of silica and NaCl at 45°C of dT on fouling. While only 14% of flux decline was observed by silica 1,000 mg/L and NaCl 25,000 mg/L, 50% of flux drop was occurred by increasing silica 5,000 mg/L. Interestingly, there was no difference between NaCl 25,000 and 45,000 mg/L in fouling ratios. It seems that there was no additional particle deposition or development of cake layers even with further increasing NaCl concentration. The influence of temperature difference (dT) on fouling is shown in Fig. 6(c). With an increase in the temperature difference, the fouling rate increased. It is likely that the fouling is accelerated by increasing the temperature difference.

3.6. Analysis of fouling behaviors by RSM

Fig. 7 presents response surfaces showing change of fouling ratios (J/J_0) (Z-axis). The graphs were drawn with change of two variables (X- and Y-axis) in fixed three conditions of the other variable. In all cases, the graph in range of more than 1.0 can be defined as no fouling. Figs. 7(a)–(c) show the effect of NaCl and feed temperature (dT) at silica concentrations of –1.68 (1,000 mg/L), 0 (5,000 mg/L), and 1.68 (9,000 mg/L). When feed contained minimum concentration of silica, no significant changes in fouling ratio are observed. This implies that low concentration of silica had a negligible effect on fouling even at high range of NaCl and dT. As shown in Figs. 7(b) and (c), fouling ratios had a decreasing tendency with two factors from medium concentration of silica and severe flux decline was caused at high concentration of silica. In Fig. 7(c), flux decreased sharply with an increase in NaCl concentration in spite of the low feed temperature condition.

Figs. 7(d)–(f) show fouling ratios as a function of silica and NaCl concentrations at different temperature conditions. In all cases, the fouling ratio increases with an increase in the temperature. When dT is –1.682 (35°C), the fouling ratios are approximately 1.0, indicating only negligible fouling occurred (Fig. 7(d)). When dT values are 0 (45°C) and 1.68 (55°C), the fouling ratio decreases with increasing silica concentration (Figs. 7(e) and (f)). The fouling ratio seems to be lowest at NaCl concentration of 0 (25,000 mg/L). These results may be attributed to the pore blocking

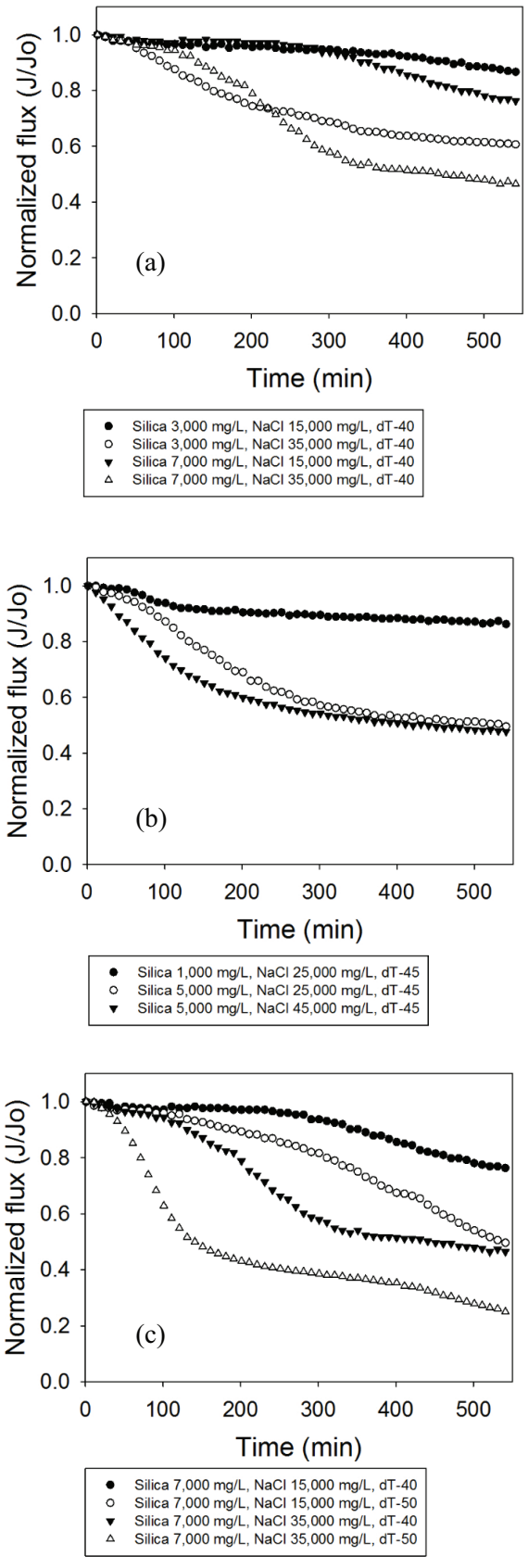

Fig. 6. Dependence of flux on time during MD experiments under various conditions.

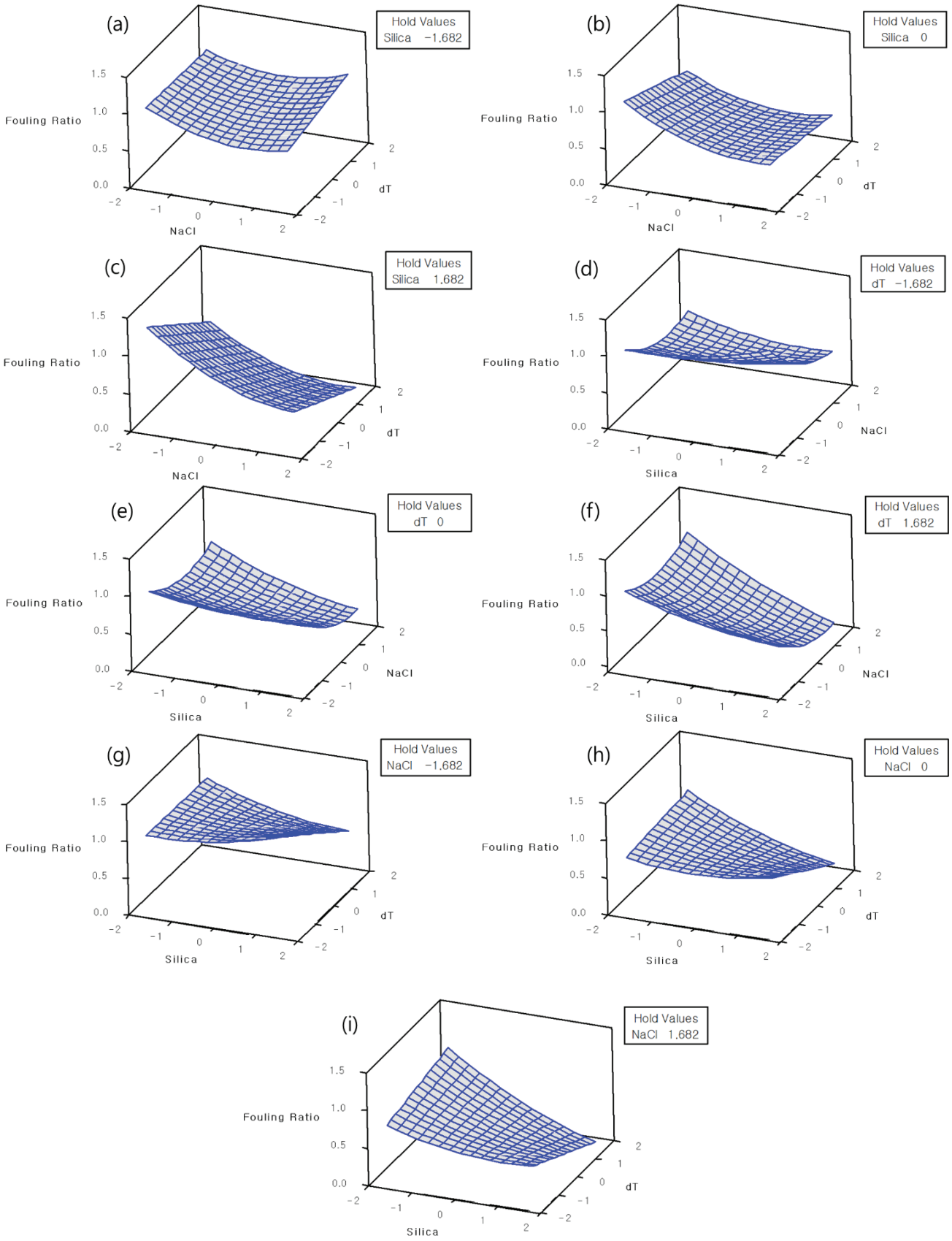

Fig. 7. RSM surfaces drawn to investigate complicate interactions between variables on membrane fouling.

mechanism [30]. In the feed formed based on ionic strength by NaCl 25,000 mg/L, most of the silica could be aggregated by the size same with membrane pore sizes (0.22 μm), leading to pore blockage. Further increase in the NaCl concentration results in the formation of larger aggregates than the pore size, leading to less severe fouling through the cake formation mechanism [30].

Figs. 7(g)–(i) present response surfaces of fouling ratios as a function of silica concentration and dT with different NaCl concentrations. At low NaCl concentration, fouling ratio is high regardless of silica concentration and dT. With an increase in NaCl concentration, the fouling ratio decreases, suggesting that NaCl is an important factor affecting the silica fouling in MD. The effect of NaCl on fouling ratio does not seem to be important under low silica concentration. However, it becomes important at high silica concentrations. In all three cases, the fouling ratio is significantly reduced by increasing dT at high silica concentrations.

4. Conclusions

In this study, silicate fouling behaviors in MD were analyzed and the following conclusions were withdrawn:

- The silica in DI water did not cause noticeable MD fouling. It is attributed to high repulsive force between colloidal silica and the membrane surface.
- The silica in NaCl solution resulted in significant flux decline due to fouling. The SEM images show thick cake layers formed on the membrane surfaces. It is likely that aggregation colloidal silica occurred at high NaCl concentrations. In addition, the temperature difference (dT) between feed and permeate accelerated MD fouling.
- RSM was applied to elucidate silica fouling in MD as a function of silica concentration, NaCl concentration, and dT. A reasonable second-order polynomial regression model was established to predict fouling ratio.
- MD fouling is found to be sensitive to silica concentration. However, a high silica concentration does not lead to severe fouling at a low NaCl concentration. In addition, a high dT does not induce fouling at a low NaCl concentration. This suggests that silica fouling in MD should be interpreted as a combined effect by silica concentration, NaCl concentration, and dT.

Acknowledgments

This research was supported by a grant (17IFIP-B065893-05) and a grant (17IFIP-B116951-02) from Industrial Facilities & Infrastructure Research Program funded by Ministry of Land, Infrastructure and Transport of Korean government.

References

[1] J. Zuo, S. Bonyadi, T.-S. Chung, Exploring the potential of commercial polyethylene membrane for desalination by membrane distillation, J. Membr. Sci., 497 (2016) 239–247.
[2] T. Husnain, Y. Liu, R. Riffat, B. Mi, Intergration of forward osmosis and membrane distillation for sustainable wastewater reuse, Sep. Purif. Technol., 156 (2015) 424–431.
[3] M.C. Fragkou, J. McEvoy, Trust matters: why augmenting water supplies via desalination may not overcome perceptual water scarcity, Desalination, 397 (2016) 1–8.
[4] M.A. Shannon, P.W. Bohn, M. Elimelech, J.G. Georgiadis, B.J. Mariñas, A.M. Mayes, Science and technology for water purification in the coming decades, Nature, 452 (2008) 301–310.
[5] P.S. Goh, T. Matsuura, A.F. Ismail, N. Hilal, Recent trends in membranes and membrane processes for desalination, Desalination, 391 (2016) 43–60.
[6] L.D. Tijing, Y.C. Woo, J.S. Choi, S. Lee, S.H. Kim, H.K. Shon, Fouling and its control in membrane distillation – a review, J. Membr. Sci., 475 (2015) 215–244.
[7] R. Bouchrit, A. Boubakri, A. Hafiane, S. Al-Tahar Bouguecha, Direct contact membrane distillation: capability to treat hypersaline solution, Desalination, 376 (2015) 117–129.
[8] A. Alkhudhiri, N. Darwish, N. Hilal, Membrane distillation: a comprehensive review, Desalination, 287 (2012) 2–18.
[9] A. Criscuoli, Improvement of the membrane distillation performance through the integration of different configurations, Chem. Eng. Res. Des., 111 (2016) 316–322.
[10] Y.Z. Tan, J.W. Chew, W.B. Krantz, Effect of humic-acid fouling on membrane distillation, J. Membr. Sci., 504 (2016) 263–273.
[11] G. Chen, Y. Lu, W.B. Krantz, R. Wang, A.G. Fane, Optimization of operating conditions for a continuous membrane distillation crystallization process with zero salty water discharge, J. Membr. Sci., 450 (2014) 1–11.
[12] A. Alhadidi, B. Blankert, A.J.B. Kemperman, J.C. Schippers, M. Wessling, W.G.J. van der Meer, Effect of testing conditions and filtration mechanisms on SDI, J. Membr. Sci., 381 (2011) 142–151.
[13] J.-S. Choi, T.-M. Hwang, S. Lee, S. Hong, A systematic approach to determine the fouling index for a RO/NF membrane process, Desalination, 238 (2009) 117–127.
[14] Y. Jin, Y. Ju, H. Lee, S. Hong, Fouling potential evaluation by cake fouling index: theoretical development, measurements, and its implications for fouling mechanisms, J. Membr. Sci., 490 (2015) 57–64.
[15] Q. She, R. Wang, A.G. Fane, C.Y. Tang, Membrane fouling in osmotically driven membrane processes: a review, J. Membr. Sci., 499 (2016) 201–233.
[16] C.H. Koo, A.W. Mohammad, F. Suja, M.Z.M. Talib, Setting-up of modified fouling index (MFI) and crossflow sampler-modified fouling index (CFS-MFI) measurement devices for NF/RO fouling, J. Membr. Sci., 435 (2013) 165–175.
[17] C. Park, H. Kim, S. Hong, S.-I. Choi, Variation and prediction of membrane fouling index under various feed water characteristics, J. Membr. Sci., 284 (2006) 248–254.
[18] A.K. Fard, T. Rhadfi, M. Khraisheh, M.A. Atieh, M. Khraisheh, N. Hilal, Reducing flux decline and fouling of direct contact membrane distillation by utilizing thermal brine from MSF desalination plant, Desalination, 379 (2016) 172–181.
[19] G. Naidu, S. Jeong, S. Vigneswaran, T.-M. Hwang, Y.-J. Choi, S.-H. Kim, A review on fouling of membrane distillation, Desal. Wat. Treat., 57 (2016) 10052–10076.
[20] P. Wang, T.-S. Chung, Recent advances in membrane distillation processes: membrane development, configuration design and application exploring, J. Membr. Sci., 474 (2015) 39–56.
[21] L.D. Nghiem, T. Cath, A scaling mitigation approach during direct contact membrane distillation, Sep. Purif. Technol., 80 (2011) 315–322.
[22] N. Javadi, F.Z. Ashtiani, A. Fouladitajar, A. Moosavi Zenooz, Experimental studies and statistical analysis of membrane fouling behavior and performance in microfiltration of microalgae by a gas sparging assisted process, Bioresour. Technol., 162 (2014) 350–357.
[23] A. Antony, J.H. Low, S. Gray, A.E. Childress, P. Le-Clech, G. Leslie, Scale formation and control in high pressure membrane water treatment systems: a review, J. Membr. Sci., 383 (2011) 1–16.
[24] D.M. Warsinger, J. Swaminathan, E. Guillen-Burrieza, H.A. Arafat, J.H. Lienhard V, Scaling and fouling in membrane distillation for desalination applications: a review, Desalination, 356 (2015) 294–313.
[25] K.S. Suganthi, K.S. Rajan, Temperature induced changes in ZnO-water nanofluid: zeta potential, size distribution and viscosity profiles, Int. J. Heat Mass Transfer, 55 (2012) 7569–7980.

[26] S.A. Khan, A. Gunther, M.A. Schmidt, K.F. Jensen, Microfluidic synthesis of colloidal silica, J. Am. Chem. Soc., 20 (2004) 8604–8611.
[27] C.Y. Tang, T.H. Chong, A.G. Fane, Colloidal interactions and fouling of NF and RO membranes: a review, Adv. Colloid Interface Sci., 164 (2011) 126–143.
[28] M. Khayet, C. Cojocaru, Artificial neural network modeling and optimization of desalination by air gap membrane distillation, Sep. Purif. Technol., 86 (2012) 171–182.
[29] Y.-J. Kim, J. Jung, S. Lee, J. Sohn, Modeling fouling of hollow fiber membrane using response surface methodology, Desal. Wat. Treat., 54 (2015) 966–972.
[30] A. Salahi, M. Abbasi, T. Mohammadi, Permeate flux decline during UF of oily wastewater: experimental and modeling, Desalination, 251 (2010) 153–160.